

Bayesian approach for limited-aperture inverse acoustic scattering with total variation prior

Xiao-Mei Yang¹, Zhi-Liang Deng^{2*} and Ailin Qian³

1. School of Mathematics, Southwest Jiaotong University, Chengdu 610031, China

2. School of Mathematical Sciences, University of Electronic Science and Technology of China, Chengdu 610054, China

3. School of Mathematical Sciences, Hubei University of Science and Technology, Xianning 437100, China

Abstract

In this work, we apply the Bayesian approach for the acoustic scattering problem to reconstruct the shape of a sound-soft obstacle using the limited-aperture far-field measure data. A novel total variation prior is assigned to the shape parameterization form. This prior is imposed on the Fourier coefficients of the parameterized form of the obstacle. Extensive numerical tests are provided to illustrate the numerical performance.

Key words: Inverse acoustic scattering; Uncertainty quantification; l_1 priors

MSC 2010: 65R32, 65R20

1 Introduction

This investigation is concerned with the 2-dimensional acoustic obstacle reconstruction problem. The goal is to detect and identify the unknown object using acoustic wave measured data. Such problem is of practical importance and has attracted a lot of interest. Over the past years, many satisfactory reconstructions have been provided [4, 6, 11]. For more references, one can refer to [6] for linear sampling method, [11, 12] for the factorization method, [9, 13] for the direct sampling method and [3, 14] for Bayesian approach. As we can see, most of these methods focus on the reconstruction problem using the full-aperture data. The limited-aperture case usually arises for example from practical difficulties in surrounding the whole region of interest by sensors. Some methods to full-aperture data and some new ideas have been developed to process the limited-aperture case, e.g., [9, 14, 15, 16, 21, 18].

*Corresponding author: dengzhl@uestc.edu.cn; Supported by Central Government Funds of Guiding Local Scientific and Technological Development for Sichuan Province No. 2021ZYD0007, NSFC No. 11601067.

Since lack of full aperture measurements, the ill-posedness and nonlinearity of the inverse problem become more severe, which makes this problem more difficult to solve. The reconstruction is not as good as the full aperture case in general [1, 8].

The present work aims at the application of the Bayesian statistical approach in the obstacle reconstruction problem, which is a further development of [14]. Our contribution in this paper is to propose a novel prior form for the unknown shape parameterization. This prior is a modified version of total variation prior. We still call it as the total variation prior (TV). Specifically, we suppose that the shape parameterization representation is expanded in Fourier series. The Fourier coefficients are assumed in the total variation prior. In [3, 14], the prior is imposed on the parameterization representation using Gaussian random field prior. Subsequently, this random field prior can be considered as a mutually independent Gaussian prior on Fourier coefficients by virtue of Karhunen-Loève expansion. In [10], we can see that the TV Markov random field prior admits advantages in designing structure priors. It is generally defined by the way of neighbor system. The TV prior in this paper is generated from the Gaussian random field prior [3, 14] by the idea in [20]. The induced parameterization representation is not as smooth as the representation from the Gaussian random field.

In the remainder, this paper is organized as follows: In Section 2, we introduce the inverse acoustic obstacle scattering problems and apply the Bayesian approach to solve it. In Section 3, a new TV prior is introduced. In Section 4, we give some numerical examples to illustrate the numerical effectiveness. Finally, the conclusions is stated.

2 Inverse Scattering Problems and Bayesian approach

We begin with the formulations of the acoustic scattering problem. Let $\Omega \subset \mathbb{R}^2$ be a bounded, simply connected domain with C^2 boundary $\partial\Omega$. Define $\mathbb{S} = \{x \in \mathbb{R}^2, |x| = 1\}$. Consider a time-harmonic plane wave propagating in the exterior of D . The velocity potential is of this form

$$U(x, t) = \text{Re} \{u^i(x)e^{-i\omega t}\} \quad \text{with } u^i(x) := e^{i\kappa x \cdot d}, \quad x \in \mathbb{R}^2, \quad d \in \mathbb{S}, \quad (2.1)$$

where d is the propagating direction, $\omega > 0$ is frequency, $\kappa = \omega/c > 0$ is the wavenumber and c is the speed of sound. Hereafter, the term $\exp(-i\omega t)$ is factored out and only the space dependent part of all waves is considered. Let D be an impenetrable sound-soft obstacle. Clearly, the obstacle will "scatter" the wave u^i so that we may write the total field as $u = u^i + u^s$, where u^s is the scattered wave. The classical physical problem is to explore the scattering phenomenon, i.e., find u^s . As we know, the scattered field u^s

is governed by an exterior boundary value problem for Helmholtz equation

$$\Delta u + \kappa^2 u = 0, \quad \text{in } \mathbb{R}^2 \setminus \bar{\Omega}, \quad (2.2a)$$

$$u = 0, \quad \text{on } \partial\Omega, \quad (2.2b)$$

$$\lim_{r \rightarrow \infty} \sqrt{r} \left(\frac{\partial u^s}{\partial r} - i\kappa u^s \right) = 0, \quad (2.2c)$$

where equation (2.2b) is the sound-soft boundary condition and (2.2c) is the Sommerfeld radiation condition.

The well-posedness of the direct scattering problem (2.2a)-(2.2c) has been established, see, e.g., [7]. We refer to the standard monograph [7] for a research statement on the significant progress both in the mathematical theories and the numerical approaches. It is well-known that the unique solution u^s of (2.2) admits an asymptotic expansion [7]

$$u^s(x, d) = \frac{e^{i\frac{\pi}{4}}}{\sqrt{8\kappa\pi}} \frac{e^{i\kappa r}}{\sqrt{r}} \left\{ u^\infty(\hat{x}, d) + \mathcal{O}\left(\frac{1}{r}\right) \right\} \quad \text{as } r := |x| \rightarrow \infty \quad (2.3)$$

uniformly in all directions $\hat{x} = x/|x|$. The function $u^\infty(\hat{x}, d)$ is called the far-field pattern. The inverse scattering problem in this paper is to find the shape of obstacle Ω from some observed far-field data. Let $\gamma^\circ \subseteq (\subsetneq) \mathbb{S}$ be the observation aperture and $\gamma^i \subsetneq \mathbb{S}$ be the incident direction. The direct scattering problem can be formulated as

$$u^\infty(\hat{x}, d) = \mathcal{F}(\Omega), \quad (\hat{x}, d) \in \gamma^\circ \times \gamma^i \quad (2.4)$$

where \mathcal{F} is the shape-to-measurement operator. If $\gamma^\circ \subsetneq \mathbb{S}$, i.e., γ° is a proper subset of \mathbb{S} , this case is referred as the limited-aperture problem. If $\gamma^\circ = \mathbb{S}$, we are concerned with the full-aperture case.

We consider a starlike obstacle Ω centering at (x_c, y_c) with boundary being parametrized as

$$\partial\Omega := (x_c, y_c) + r(\theta)(\cos \theta, \sin \theta) = (x_c, y_c) + \exp(q(\theta))(\cos \theta, \sin \theta), \quad (2.5)$$

where $q(\theta) = \log r(\theta)$, $0 < r(\theta) < r_{\max}$, $\theta \in [0, 2\pi)$. With the parameterization, we take the noise in measurements into account and rewrite (2.4) as a statistical inference model

$$y = \mathcal{F}(q) + \eta, \quad (2.6)$$

where $q \in X$ and $y = u_\infty(\hat{x}, d) \in Y$ for some suitable Banach spaces X and Y , respectively. In particular, y is the noisy observations of $u^\infty(\hat{x}, d)$ and $\eta(\hat{x}, d)$ is the noise. In this paper, we assume that the observation noise is normal with mean zero and independent of q , i.e., $\eta(\hat{x}, d) \sim \mathcal{N}(0, \sigma^2(\hat{x}))$.

Apart from mere estimation purposes, a major goal of statistical inference is to find the posterior distribution $p(q|y)$. Bayes Theorem provides a

principled way for calculating the posterior conditional probability. According to Bayes' formula, it has the following representation

$$p(q|y) = \frac{p(y|q)p(q)}{p(y)} \propto p(y|q)p(q), \quad (2.7)$$

where $p(y|q)$ is the likelihood, $p(q)$ is the prior and $p(y)$ is the normalized constant. The likelihood model is established by the forward model and noise model. And it admits by (2.6)

$$p(y|q) \propto \exp\left(-\frac{\|\mathcal{F}(q) - y\|^2}{2\sigma^2}\right) := \exp(-\Phi(q, y)). \quad (2.8)$$

The prior model provides the prior knowledge for the unknown parameters before the data is collected. We will discuss it in the subsequent section. One also can refer to [2, 5, 19] for more details.

The Bayesian approach answers richer questions than the traditional regularization-based methodologies. As we can see, the solution it produces is not limited to individual values but consists of probability distributions. Therefore, it provides an effective tool to analyze the relative probabilities of different approximate solutions or the probability of a solution to lie in a subset of the solution space for decision maker.

3 Total variation prior

A key sticking point of Bayesian analysis is the prior elicitation, which usually plays a defining role in Bayesian statistical inference. There is a vast literature on the related discussion, e.g., [17, 10, 20]. A rich class of prior distributions can be derived from the theory of Markov random fields (MRF), which is usually defined in the discrete form by the neighborhood system [2, 10, 20]. In this paper, the prior for q is taken as the Gauss MRF $N(0, \Gamma)$ with covariance operator $\Gamma = Q^{-1}$. Here Q is the precision operator defined by the fractional diffusion operator $-(\frac{d^2}{d\theta^2})^s$ with periodic boundary condition.

In real numerical implementation, we need the discrete form of a random variate. There are two ways to transform the infinite dimensional random variate into its finite pattern. In the first way, we take a mesh partition $\tilde{\Omega}$. Denote the discretized version of precision operator Q by \mathbf{Q} . The discretize can be done by the finite difference, finite element etc. The joint density function for $\mathbf{q} := [q(\theta_1), q(\theta_2), \dots, q(\theta_m)]^\top$ is Gaussian and admits the form

$$p(\mathbf{q}) = (2\pi)^{-m/2} |\mathbf{Q}|^{1/2} \exp(-\frac{1}{2} \mathbf{q}^\top \mathbf{Q} \mathbf{q}). \quad (3.1)$$

In this way, the finite dimensional samples of q can be generated by the probability distribution (3.1). Denote eigenvalues and eigenvectors of precision matrix \mathbf{Q} by $\lambda_{\mathbf{Q}}$ and $q_{\mathbf{Q}}$. In the second way, we use the Karhunen-Loève

expansion to represent the prior random variate. The precision operator Q admits eigenvalues λ_k and eigenfunctions ψ_k , $k = 1, 2, \dots$, i.e.,

$$Q\psi_k = \lambda_k\psi_k, \quad k = 1, 2, \dots. \quad (3.2)$$

According to Karhunen-Loève expansion of q , we have

$$q(x) = \sum_{k=1}^{\infty} \frac{B_k}{\lambda_k} \psi_k(x) \approx \sum_{k=1}^m \frac{B_k}{\lambda_k} \psi_k(x) := \tilde{q}(x), \quad (3.3)$$

where B_k s are independent identity distribution normal Gaussian. The truncated form $\tilde{q}(x)$ is used in the numerical implement process.

In fact, it can be verified that λ_Q behaves like λ_k and θ_Q s are vectors of values of ψ_k at discrete points. Based on this reason, in our numerical test, we do not distinguish them any more. And in the subsequent parts, we only use the KL expansion to represent the prior. Therefore, the prior for the unknown q is determined by its expansion coefficients B_k s.

Remark 1. In the KL expansion prior condition, we actually assume the function $q(\theta)$ admits Fourier series representation

$$q(\theta) = \sum_{k=1}^{\infty} B_k \psi_k(\theta). \quad (3.4)$$

And the prior for B_k is given by $N(0, \frac{1}{\lambda_k^2}I)$ from (3.3).

For a Gaussian random vector with mutually independent components, we may transform it to an l_1 -type prior according to the theories in [20]. For this purpose, an invertible mapping function $g: \mathbb{R} \rightarrow \mathbb{R}$ is introduced

$$g(B_k) \equiv \mathcal{L}^{-1}(\mathcal{G}(B_k)) = -\frac{1}{\lambda} \text{sign}(B_k) \log(1 - |2\mathcal{G}(B_k) - 1|), \quad (3.5)$$

where \mathcal{L} is the cumulative distribution function (cdf) of the Laplace distribution and \mathcal{G} is the cdf of the standard Gaussian distribution. This function g relates a Gaussian reference random variable $B_k \in \mathbb{R}$ to the Laplace-distributed parameter $A_k \in \mathbb{R}$, such that $A_k = g(B_k)$. Then we apply the transformation to each components of B

$$A(B) := [g(B_1), g(B_2), \dots, g(B_m)]^\top. \quad (3.6)$$

A prior transformation for the l_1 -type prior is $Z_q := D^{-1}A(B)$, i.e.,

$$p(Z_q) \propto \exp(-\lambda|DZ_q|) = \exp(-\lambda \sum_{i=1}^m |DZ_q|_i), \quad (3.7)$$

where D is an invertible matrix. For total variation prior, the invertible matrix D is taken as [20]

$$D_0 = \begin{bmatrix} 1 & & & 1 \\ -1 & 1 & & \\ & \ddots & \ddots & \\ & & -1 & 1 \end{bmatrix}_{m \times m}. \quad (3.8)$$

We use a modified version of D_0 as $D = I + \alpha D_0$ with a small constant $\alpha_0 > \alpha > 0$. By this, we actually take $|DZ_q|$ in (3.7) as

$$|DZ_q| = |(1 + \alpha)z_1 + \alpha z_m| + \sum_{i=2}^m |z_i + \alpha(z_i - z_{i-1})|, \quad (3.9)$$

where z_i is the i -th component of Z_q . Since D is nonsingular matrix, (3.9) defines a norm of vector Z_q . Therefore, it follows that the norm in (3.9) is equivalent to the normal norm.

Remark 2. The total variation strengthens the relatedness of the Fourier coefficients. In (3.3), the Fourier coefficients are required to be independent. However, the convergence of Fourier series actually implies that they are not completely uncorrelated. Though we here can not use the total variation prior to reflect the convergence, the correlation of Fourier coefficients is added.

4 Numerical examples

We use the pCN Markov chain Monte Carlo algorithm [19] listed in Algorithm 1 to implement the sampling process. We take several benchmark examples in acoustic obstacle scattering to verify the numerical effectiveness ($\theta \in (0, 2\pi]$), see Table 1.

The true data is generated by solving the forward problem by boundary integral equation method [7]. Let ϕ be the observation angle such that $\hat{x} := (\cos \phi, \sin \phi)$. We use the observation/measurement apertures as follows:

$$\begin{aligned} \gamma_1^o &= \{(\cos \phi, \sin \phi) \mid \phi \in [0, 2\pi]\}, \\ \gamma_2^o &= \{(\cos \phi, \sin \phi) \mid \phi \in [0, \pi]\}, \\ \gamma_3^o &= \{(\cos \phi, \sin \phi) \mid \phi \in [0, \pi/2]\}. \end{aligned}$$

The incident apertures are

$$\begin{aligned} \gamma_1^i &= \{(1, 0)\}, \\ \gamma_2^i &= \{(\cos \theta, \sin \theta) \mid \theta = \{\pi/2, 3\pi/2\}\}. \end{aligned}$$

The relative noise is added to the true data by

$$y = u^\infty(\hat{x}, d) + (\eta_1 + \eta_2 i) \|u^\infty(\hat{x}, d)\|_\infty. \quad (4.1)$$

Algorithm 1 pCN MCMC algorithm

- 1: Initialize: Pick B^0 . Promote B^0 to Z_q^0 according to (3.6)-(3.8) and compute $\tilde{q}(Z_q^0)$ by (3.3). Set $j = 0$.
- 2: While $j < N$, continue:

- Draw a proposal \hat{B} according to

$$\hat{B} = \sqrt{1 - \beta^2} B^j + \beta B_{\text{pr}},$$

where $B_{\text{pr}} \sim N(0, I)$ and $\beta \in (0, 1)$ is a constant. Transform \hat{B} to \hat{Z}_q according to (3.6)-(3.8). Generate $\tilde{q}(\hat{Z}_q)$ using (3.3) with coefficients \hat{Z}_q .

- Compute the acceptance probability:

$$\alpha = \min \left\{ 1, \frac{\exp \left(-\Phi(\tilde{q}(\hat{Z}_q), g) \right)}{\exp \left(-\Phi(\tilde{q}(Z_q^j), g) \right)} \right\}.$$

- Flip an α -coin: Draw $\xi \sim \text{Uniform}([0, 1])$:
 - If $\xi \leq \alpha$, accept the proposal, setting $B^{j+1} = \hat{B}$,
 - else, reject the move and stay put $B^{j+1} = B^j$.
 - Increase $j \leftarrow j + 1$.
-

Table 1: The boundary parameterizations of the object obstacles

Kite	$(x_1, x_2) = (\cos \theta + 0.65 \cos 2\theta - 0.65, 1.5 \sin \theta)$
Roundrect	$r(\theta) = (\cos^4 \theta + (2/3 \sin \theta)^4)^{-1/4}$
Acorn	$r(\theta) = \frac{3}{5} \sqrt{\frac{17}{4} + 2 \cos 3\theta}$
Pear	$r(\theta) = \frac{5 + \sin 3\theta}{6}$
Bean	$r(\theta) = 0.4 \sqrt{4 \cos^2 \theta + \sin^2 \theta}$
Threelobes	$r(\theta) = 0.5 + 0.25 \exp(-\sin 3\theta) - 0.1 \sin \theta$
Star	$r(\theta) = 1 + 0.3 \sin 5\theta$
Cloverleaf	$r(\theta) = 1 + 0.3 \cos 4\theta$
Peanut	$r(\theta) = 0.4 \sqrt{4 \cos^2 \theta + \sin^2 \theta}$
Drop	$(x_1, x_2) = (-1 + 2 \sin(\theta/2), -\sin \theta)$

In these numerical tests, we fix some parameters in the prior, $s = 2.2$, $\lambda = 0.2$, $\alpha = 0.1$. The Fourier expansion of q is truncated to the first 27 terms. The wave number is set to $\kappa = 1$. The true center position (x_c, y_c) is fixed at $(0, 0)$. And we take the samples after 1000 iteration and use the mean estimation as the approximation of the unknown parameters.

We first consider the cases of one incident wave and two incident waves, i.e., $\gamma^i = \gamma_1^i$ and $\gamma^i = \gamma_2^i$, with full observation aperture. Taking one observation aperture with γ_1^o , we display the numerical reconstructions in Fig. 1 ($\gamma^o \times \gamma^i = \gamma_1^o \times \gamma_1^i$), Fig. 2 ($\gamma^o \times \gamma^i = \gamma_1^o \times \gamma_2^i$) using noise level $\eta_1 = 1\%$, $\eta_2 = 1\%$, respectively. The results show that the two incident waves perform better. In the following tests, we use two incident waves case.

The limited aperture cases are then considered with the same noise configuration in the full aperture cases. In Fig. 3, we show the numerical reconstructions using observation aperture $\gamma^o = \gamma_2^o$ with two incident waves, i.e., $\gamma^o \times \gamma^i = \gamma_2^o \times \gamma_2^i$. With smaller observation aperture $\gamma^o = \gamma_3^o$, Fig. 4 shows the reconstructions for two incident waves $\gamma^i = \gamma_2^i$. The results show that the reconstructions are satisfactory for more observation data. When observation aperture becomes small, the reconstructions get worse.

We also check the numerical accuracy using inaccurate center positions

(x_c, y_c) in the reconstruction process. We use the following 8 different centers, (see Fig. 5 (a))

$$(\pm 0.2, \pm 0.2), (0, \pm 0.2), (\pm 0.2, 0),$$

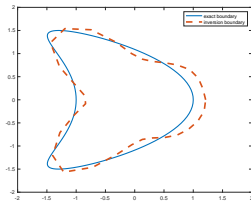
to reconstruct the Kite shape. The reconstructions are displayed In Fig. 5 (b). From the displayed results, we can conclude that even the center is not exact, the reconstruction has not been seriously affected. This means that if we can use some method, e.g., the extended sampling method [14], to find the approximated center first, the proposed method will provide satisfactory reconstruction.

5 Conclusions

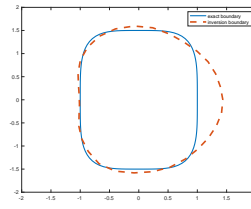
We discuss the application of the Bayesian method for the limited aperture inverse scattering problem. A novel total variation prior is proposed for the shape parameterization representation. Numerical examples show that the proposed method with the prior can yield satisfactory reconstructions even when the measurement data is quite limited.

References

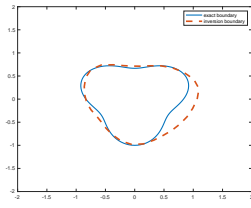
- [1] L. Audibert and H. Haddar. The generalized linear sampling method for limited aperture measurements. *SIAM Journal on Imaging Sciences*, 10(2):845–870, 2017.
- [2] Johnathan M. Bardsley. Gaussian markov random field priors for inverse problems. *Inverse Problems and Imaging*, 7(2):397–416, 2013.
- [3] T. Bui-Thanh and O. Ghattas. An analysis of infinite dimensional bayesian inverse shape acoustic scattering and its numerical approximation. *SIAM/ASA Journal on Uncertainty Quantification*, 2(1):203–222, 2014.
- [4] F. Cakoni and D. Colton. *A Qualitative Approach in Inverse Scattering Theory*, volume AMS Vol. 188. Springer-Verlag.
- [5] D. Calvetti and E. Somersalo. Inverse problems: From regularization to bayesian inference. *WIREs Computational Statistics*, 10(3):1–19, 2018.
- [6] D. Colton and A. Kirsch. A simple method for solving inverse scattering problems in the resonance region. *Inverse Problems*, 12:383–393, 1996.
- [7] D. Colton and R. Kress. *Inverse Acoustic and Electromagnetic Scattering Theory*. Springer-Verlag, Berlin, 3rd edition edition, 2013.



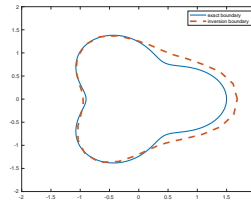
(a) Kite



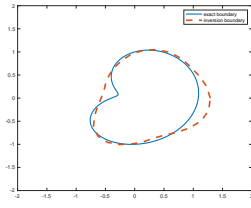
(b) Roundrect



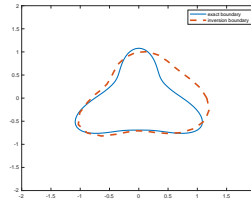
(c) Pear



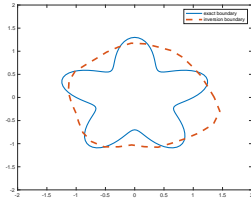
(d) Acorn



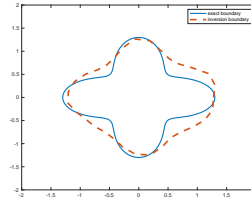
(e) Bean



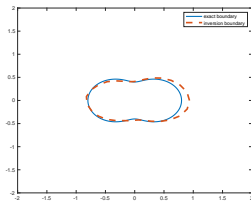
(f) Threelobes



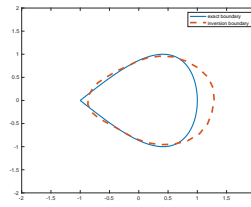
(g) Star



(h) Cloverleaf

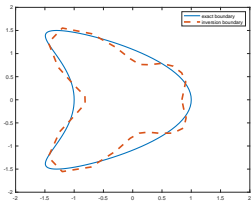


(i) Peanut

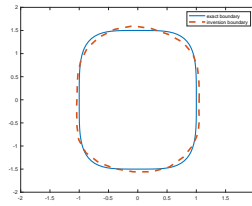


(j) Drop

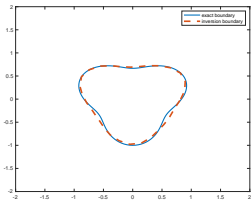
Figure 1: Reconstructions for different shapes using $u^\infty(\hat{x}, d)$, $(\hat{x}, d) \in \gamma_1^o \times \gamma_1^i$ with $\eta_1 = 1\%$, $\eta_2 = 1\%$.



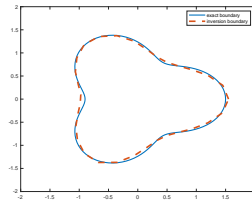
(a) Kite



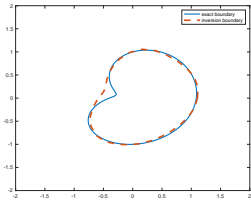
(b) Roundrect



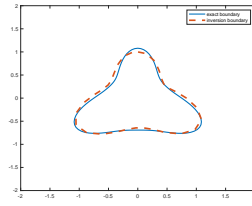
(c) Pear



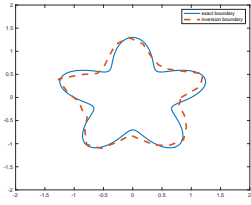
(d) Acorn



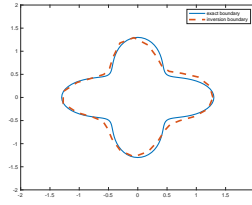
(e) Bean



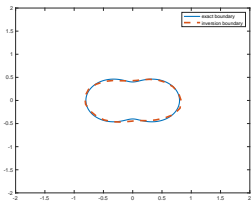
(f) Threelobes



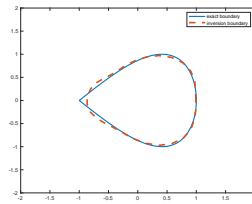
(g) Star



(h) Cloverleaf



(i) Peanut



(j) Drop

Figure 2: Reconstructions for different shapes using $u^\infty(\hat{x}, d)$, $(\hat{x}, d) \in \gamma_1^o \times \gamma_2^i$ with $\eta_1 = 1\%$, $\eta_2 = 1\%$.

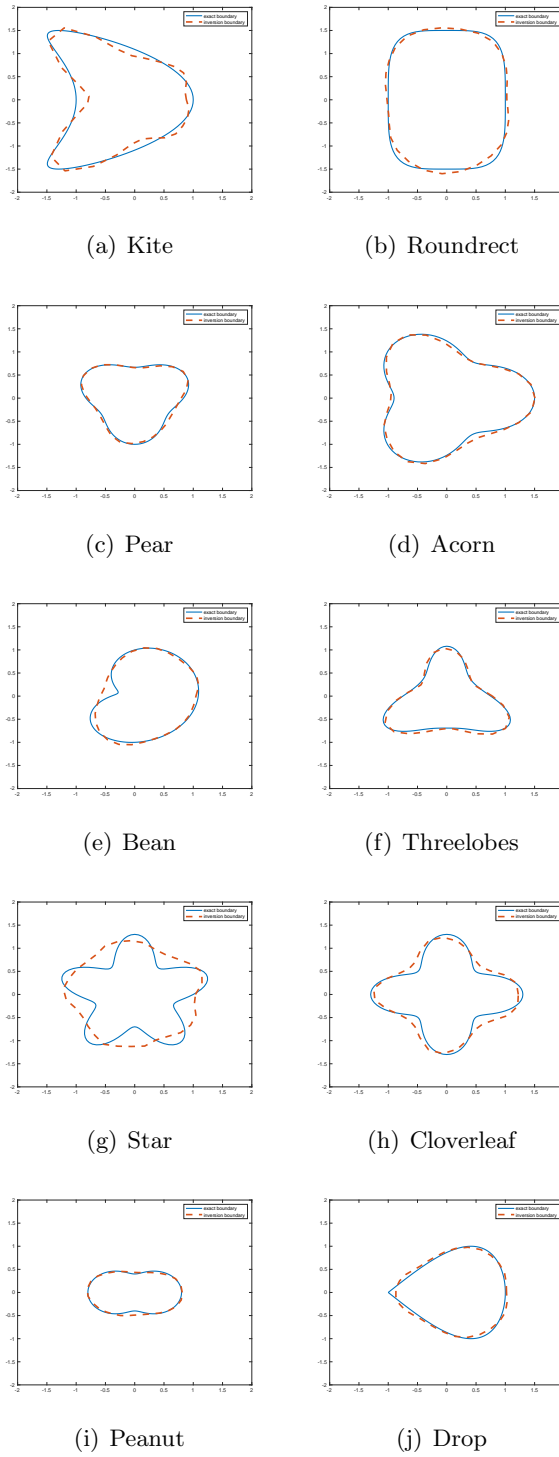


Figure 3: Reconstructions for different shapes using $u^\infty(\hat{x}, d)$, $(\hat{x}, d) \in \gamma_2^o \times \gamma_2^i$ with $\eta_1 = 1\%$, $\eta_2 = 1\%$.

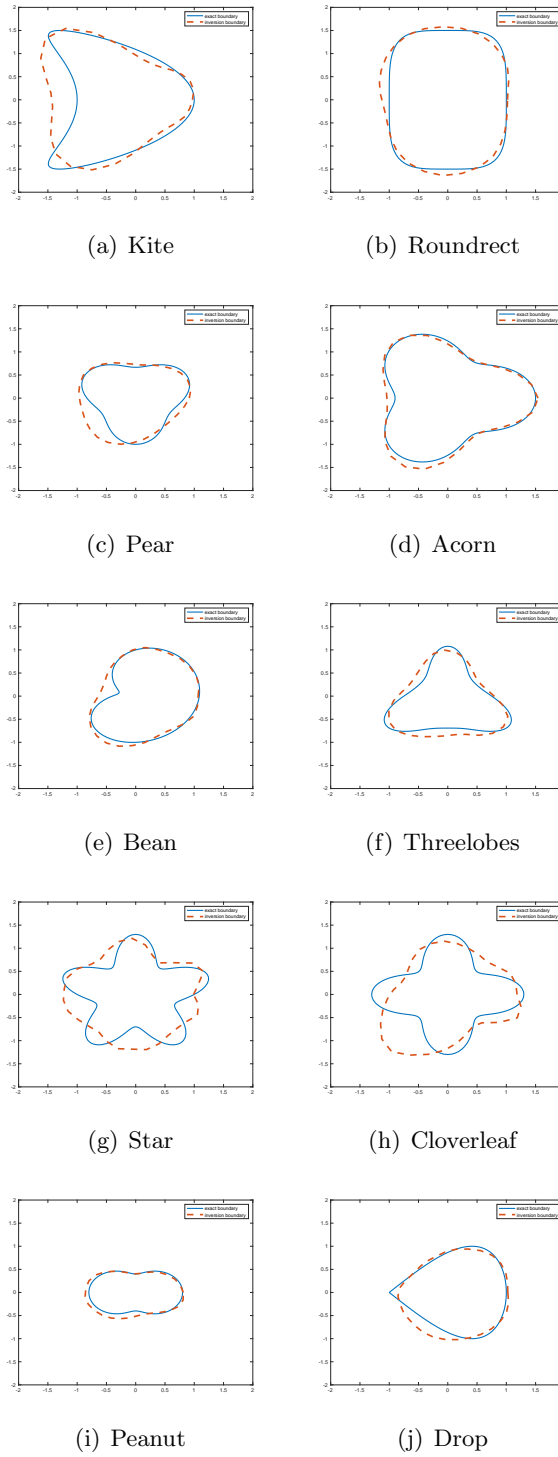


Figure 4: Reconstructions for different shapes using $u^\infty(\hat{x}, d)$, $(\hat{x}, d) \in \gamma_3^0 \times \gamma_2^1$ with $\eta_1 = 1\%$, $\eta_2 = 1\%$.

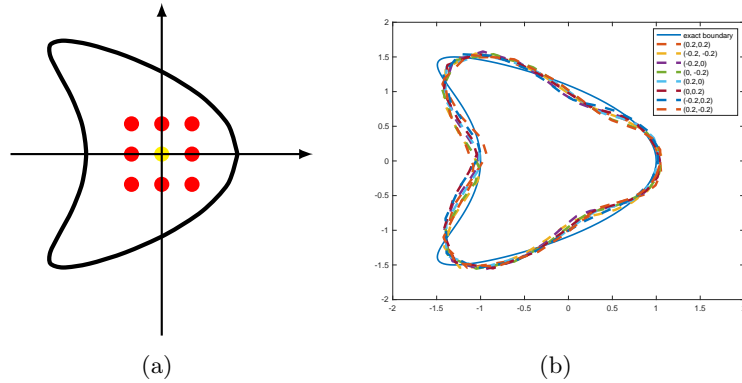


Figure 5: (a) Center points: Yellow dot is the true center position; Red dots are the center positions used in the reconstruction; (b) Reconstructions for Kite shape using 8 different centers with $(\hat{x}, d) \in \gamma_1^o \times \gamma_2^i$, $\eta_1 = 1\%$, $\eta_2 = 1\%$.

- [8] Y. Guo, P. Monk, and Colton. The linear sampling method for sparse small aperture data. *Applicable Analysis*, 95(8):1599–1615, 2016.
- [9] B. Jin K. Ito and J. Zou. A direct sampling method to an inverse medium scattering problem. *Inverse Problems*, 28(025003), 2012.
- [10] Jari P. Kaipio and Erkki Somersalo. *Statistical and Computational Inverse Problems*, volume 160. Springer, 1 edition, 2005.
- [11] A. Kirsch. Charaterization of the shape of a scattering obstacle using the spectral data of the far field operator. *Inverse Problems*, 14:1489–1512, 1998.
- [12] A. Kirsch and N. Grinberg. *The Factorization Method for Inverse Problems*. Oxford University Press, 2008.
- [13] J. Li and J. Zou. A direct sampling method for inverse scattering using far-field data. *Inverse Problems and Imaging*, 7:757–775, 2013.
- [14] Z. Li, Z. Deng, and J. Sun. Extended-sampling-bayesian method for limited aperture inverse scattering problems. *SIAM Journal on Imaging Sciences*, 13(1):422–444, 2020.
- [15] J. Liu and J. Sun. Extended sampling method in inverse scattering. *Inverse Problems*, 34(8):085007, 2018.
- [16] X. Liu and J. Sun. Data recovery in inverse scattering: from limited-aperture to full-aperture. *J. Comput. Phys*, 386:350–364, 2019.
- [17] Ali Mohammad-Djafari. Bayesian approach with prior models which enforce sparsity in signal and image processing. *EURASIP Journal on Advances in Signal Processing*, 52, 2012.

- [18] R. Potthast. A survey on sampling and probe methods for inverse problems. *Inverse Problems*, 22(2):R1–R47, 2006.
- [19] Andrew M. Stuart. Inverse problems: A bayesian perspective. *Acta Numerica*, 19:451–559, 2010.
- [20] Zheng Wang, Johnathan M. Bardsley, Antti Solonen, Tiangang Cui, and Youssef M. Marzouk. Bayesian inverse problems with l_1 priors: A randomize-then-optimize approach. *SIAM Journal on Scientific Computing*, 39(5), 2017.
- [21] A. Zinn. On an optimisation method for the full- and limited-aperture problem in inverse acoustic scattering for a sound-soft obstacle. *Inverse Problems*, 5:239–253, 1989.